Two-stage processing of aesthetic information in the human brain revealed by neural adaptation paradigm

Miho Iwasaki[1], and Yasuki Noguchi[1,*,] and Ryusuke Kakigi[2]

[1]Department of Psychology, Graduate School of Humanities, Kobe University, 1-1 Rokkodai-cho, Nada, Kobe, 657-8501, Japan.

[2]Department of Integrative Physiology, National Institute for Physiological Sciences, 38 Nishigonaka, Myodaiji, Okazaki, 444-8585, Japan

* Corresponding author. E-mail: ynoguchi@lit.kobe-u.ac.jp

Number of figures: 5 (no table),

Abstract

Some researchers in aesthetics assume visual features related to aesthetic perception (e.g. golden ratio and symmetry) commonly embedded in masterpieces. If this is true, an intriguing hypothesis is that the human brain has neural circuitry specialized for the processing of visual beauty. We presently tested this hypothesis by combining a neuroimaging technique with the repetition suppression (RS) paradigm. Subjects (non-experts in art) viewed two images of sculptures sequentially presented. Some sculptures obeyed the golden ratio (canonical images), while the golden proportion were impaired in other sculptures (deformed images). We found that the occipito-temporal cortex in the right hemisphere showed the RS when a canonical sculpture (e.g. *Venus de Milo*) was repeatedly presented, but not when its deformed version was repeated. Furthermore, the right parietal cortex showed the RS to the canonical proportion even when two sculptures had different identities (e.g. *Venus de Milo* as the first stimulus and *David di Michelangelo* as the second), indicating that this region encodes the golden ratio as an abstract rule shared by different sculptures. Those results suggest two separate stages of neural processing for aesthetic information (one in the occipito-temporal and another in the parietal regions) that are hierarchically arranged in the human brain.

Key words: repetition suppression, neuroaesthetics, magnetoencephalography (MEG), golden ratio

Introduction

Neuroaesthetics is a growing field of cognitive and affective neuroscience (Cela-Conde et al. 2011; Chatterjee and Vartanian 2014; Di Dio and Gallese 2009; Nadal and Pearce 2011; Zeki 1999). Although issues on aesthetics (e.g. definitions of beauty and aesthetic experiences) have been traditionally discussed in the field of humanities, neuroscientists and neuropsychologists recently approached this issue in a scientific way, such as using functional magnetic resonance imaging (fMRI), electroencephalography (EEG), and magnetoencephalography (MEG). Those approaches have provided some insight into neural mechanisms of our brain for perception and production of art (Jacobsen 2013; Nadal 2013; Vessel et al. 2013).

One of most debated issues in aesthetics is whether an appreciation of beauty depends on subjective factors (preferences and personal values of viewers) or it can be associated with sensory features embedded in stimuli (shapes, colors, and proportions of artworks) (Di Dio et al. 2007). The former (subjective) view is consistent with daily experiences that aesthetic preferences and evaluations greatly vary among different individuals. Indeed, many studies have indicated that appreciations of artworks are highly subjective, depending on viewers' values, experiences, and knowledge on art (Hekkert and VanWieringen 1996; Winston and Cupchik 1992). On the other hand, some other studies have explored sensory parameters (features) of stimuli that are shared by beautiful things. A representative one is symmetry of visual images. It is known that symmetric pictures are more judged to be beautiful than asymmetric ones (Jacobsen et al. 2006). Another candidate for visual beauty would be a proportion of stimulus. In case of sculptures representing human bodies, a foot-to-navel: navel-to-head proportion of 1: 0.618 is called the golden ratio (Di Dio et al. 2007; Livio 2003) and is considered to be the canonical proportion commonly embedded in many masterpieces. Although the golden ratio was originally a beauty ideal of western culture, it is now reported

that many people in Japan (eastern Asia) were also sensitive to this ratio, showing a preference to objects obeying the canonical section and proportion (Nakamura 2002; Noguchi and Murota 2013).

An effective approach to seek evidence for visual beauty is to investigate how the human brain reacts to those features of beauty. For example, if we find a rapid (reflexive) and selective neural response to a visual stimulus with symmetry or the golden ratio, especially from brains of people with no professional knowledge or education of art (non-experts), this would suggest a neural mechanism in our brain that detects and processes visual beauty. Di Dio et al. (2007) tested this possibility by manipulating proportions of sculpture images. They used fMRI and measured hemodynamic signals of non-experts' brain induced by two sets of images, one consisting of original (prototype) sculptures with a proportion of the golden ratio and the other consisting of modified (deformed) versions of those images. The two sets of sculpture images looked similar but critically different only in terms of a presence/absence of visual beauty (proportion). They found increased neural responses to the original than deformed stimuli in the insula, precuneus, and prefrontal regions, etc. This experimental design comparing brain responses to prototype (art) vs. deformed (non-art) stimuli has been also used in later studies (Lacey et al. 2011; Mizokami et al. 2014; Noguchi and Murota 2013).

Results of those studies suggested neural circuitry or brain regions activated by aesthetic information. One should note, however, that those regions were identified through a contrast between stimuli with beauty (e.g. sculptures with a canonical proportion) and those without it (e.g. sculpture with a distorted proportion). They looked similar but were not identical. It thus remained unclear whether differential brain responses to the two types of stimuli resulted from a presence/absence of visual beauty or simply reflected differences in

visual inputs. To clarify this point, visual inputs should be thoroughly controlled between experimental and control conditions.

In the present study, we addressed this issue using the neural adaptation technique (Buckner et al. 1998; Grill-Spector et al. 1999; Henson et al. 2000; Kourtzi and Kanwisher 2001; Miller et al. 1991; Wiggs and Martin 1998), an established paradigm in the field of electrophysiology and neuroimaging. A key point of this paradigm is that neurons (or brain regions) show suppression in their response to repeatedly-presented stimuli or the information to which they are sensitive (Barron et al. 2016), a phenomenon called the repetition suppression (RS). Although the RS was originally reported in the sensory cortex, an experimental paradigm using the RS has been now applied to a wide variety of tasks involving high-level neural processes, such as language (Gagnepain et al. 2008), time perception (Hayashi et al. 2015), and social cognition (Jenkins et al. 2008; Lau and Cikara 2017). As shown in **Figure 1A**, all trial in the current study involved two images of sculptures (S1 and S2) sequentially presented in the central visual field. A sculpture with the canonical proportion was repeatedly presented in one condition (e.g. same-sculpture same-proportion or S-S trials, **Fig. 1B**), while only S2 had the canonical proportion in another condition (e.g. same-sculpture different-proportion or S-D trials). We predicted that brain regions processing the information of the canonical proportion would show a reduced response to S2 in S-S than S-D conditions, because a stimulus with the canonical proportion is repeated in S-S trials. A major advantage of this paradigm is that we can completely control visual inputs between critical conditions (Noguchi et al. 2004). In both S-S and S-D trials, the same sculpture image with the golden ratio was presented as S2 (e.g. *David di Michelangelo*), which eliminated a possibility that differential S2 responses between S-S and S-D trials resulted from the differences in visual inputs (spatial frequency and luminance contrast, etc.) of those conditions.

One important feature of visual beauty is that it is shared by many artworks (generality). If there is a certain brain region reacting to a sculpture with the canonical proportion, it would also respond to another sculpture sharing the same rule of beauty. To explore such regions encoding visual beauty in a general manner, we set two additional conditions in which sculptures with different identities were used as S1 and S2 (e.g. *Venus de Milo* as S1 and *David di Michelangelo* as S2, **Fig. 1A**). In one condition, both of the sculptures obeyed the golden ratio (different-sculpture same-proportion or D-S trials), while only S2 had the canonical proportion in another condition (different-sculpture different-proportion or D-D trials). A comparison of neural responses to S2 between D-S and D-D trials would reveal brain regions reacting to visual beauty in a general (identity-independent) manner.

We currently used MEG to measure brain activity of non-expert subjects. The advantages of MEG are two-fold. First, we can record neural activity induced by S1 and S2 separately. To induce the robust RS, an inter-stimulus interval (ISI) between S1 and S2 should be as short as possible. A fine temporal resolution of MEG allowed us to measure responses to each sculpture even with such short ISIs. Second, in addition to locations of brain areas related to aesthetic perception, we can know through MEG measurements when those areas are activated by the canonical proportion. Such information about the latency of neural activity would help us to know how quickly the human brain can react to visual features related to aesthetic perception.

Materials and Methods

Participants

Twenty adults participated in the present study (seven males and thirteen females, mean age: 27.68). This number of participants was comparable to or larger than those in prior studies (14-20) (Cela-Conde et al. 2009; Cupchik et al. 2009; Di Dio et al. 2007; Jacobsen et al. 2006;

Kawabata and Zeki 2004; Kirk et al. 2009; Noguchi and Murota 2013). All subjects were Asian (native speakers of Japanese) and had normal or corrected-to-normal visual acuity. According to the Edinburgh Handedness Inventory (Oldfield 1971), all subjects were right handed (Laterality Quotient or LQ: 0.667 – 1.000) except for two left-handed (LQ: -0.059 and -0.500) and one ambidextrous (LQ: 0) subjects. Informed consent was received from each participant after the nature of the study had been explained. All experiments were carried out in accordance with guidelines and regulations approved by the ethics committee of Kobe University and the National Institute for Physiological Sciences, Japan.

Stimuli and task

All visual images were generated and presented through the Matlab Psychophysics Toolbox (Brainard 1997; Pelli 1997). Detailed information about sculpture images was shown in our previous study (Noguchi and Murota 2013). Briefly, we used images of 26 artworks of the Classical and Renaissance periods (e.g., *Doryphoros* by *Polykleitos*). These sculptures met the criteria of the golden ratio and were characterized by the canonical foot-to- navel: navel-to-head proportion of 1: 0.60–0.63. Images of non-canonical (deformed) sculptures, on the other hand, were made by applying two types of deformation to those canonical images, one into a short-leg (long-trunk) proportion (1: 0.64–0.82) and another into a long-leg (short-trunk) proportion (1: 0.45–0.59).

Structures of one trial are shown in **Figure 1A**. Each trial started with a fixation screen of 0.4 s, followed by a presentation of a first sculpture image (S1, 0.5 s). After an inter-stimulus interval of 0.4 – 0.6 s (variable across trials), we presented a second sculpture image (S2) for 0.5 s. At the end of each trial, subject made an aesthetic judgment on the S2 images using a five-point scale (Kirk et al. 2009) from 1 (very unappealing) to 5 (very appealing). We instructed subjects to neglect the S1 images, because those images were not

relevant to the task. They were not informed about a distortion of a proportion applied to a subset of stimuli. No time limitation was imposed for this aesthetic rating task.

We set five types of trials randomly intermixed within each experimental session. Structures of those five conditions are summarized in **Figure 1B**. In the first type of trials, an identical image with the canonical proportion was repeatedly shown as S1 and S2 (the same-sculpture same-proportion or S-S condition). The canonical image of S1 was replaced by the deformed version (either with a short-leg or long-leg proportion) of the same sculpture in the second type of trials (same-sculpture different-proportion or S-D condition). On the other hand, we presented images of two different sculptures in the third and fourth conditions. Both S1 and S2 in the third (D-S) condition had the canonical proportion, while a proportion of S1 was deformed in the fourth (D-D) condition. Finally, we tested the lowest control condition in which an identical sculpture with a deformed proportion was repeatedly presented as S1 and S2 (S-S-def).

Note that the first four conditions from S-S to D-D involved the S2 with the canonical proportion. Differential neuromagnetic responses induced by S2 image (e.g. *David di Michelangelo*) thus would reflect a contextual modulation of S2 by S1 (i.e. RS), rather than low-level visual properties of S2 image such as luminance contrast and spatial frequency. For example, reduced MEG responses to S2 in S-S compared to S-D conditions (S-S-2 < S-D-2) would be caused by a repetition of same visual image (visual RS) or a repetition of the canonical proportion (proportion-based RS). Each experimental session comprised 65 trials (13 trials for each condition) and subject performed six sessions. We showed in **Fig. 1C** an assignment of the 26 sculpture images in S2 over the six sessions.

MEG recordings and analyses

Neural response to S1 and S2 images were recorded with a whole-head 306-channel MEG

system (Vector-view, ELEKTA Neuromag, Helsinki, Finland), which measured changes in neuromagnetic signals from 102 sensor positions over the scalp. A sensor element at each position was composed of one magnetometer and two orthogonal planar-type gradiometers (one for latitudinal and another for longitudinal directions of changes in neuromagnetic signals). In the present study, we analyzed MEG signals recorded from 204 gradiometers at 102 sensor positions. Signals of those gradiometers are less sensitive to global noise (e.g. ones induced by body movements and geomagnetism) and mainly reflect local neuromagnetic response from the cerebral cortex just below a sensor position (Nishitani and Hari 2002). To avoid the noise caused by eye movements and blinks, we instructed subjects not to move their eyes while S1 and S2 were displayed on the screen, although they were allowed to move their eyes freely during the aesthetic rating.

The MEG signals were recorded with an analog band-pass filter of 0.1–330 Hz and digitized at 1,000 Hz. We investigated neural response to sculpture images by computing visual-evoked fields (VEFs) separately for S1 and S2. An epoch for an across-trial averaging ranged from 100 ms before to 750 ms after an onset of S1 or S2, with an initial 100 ms (pre-stimulus period) used as a baseline. Epochs with a peak-to-peak signal variation larger than 3000 fT/cm were excluded from the averaging (Noguchi et al. 2004).

To evaluate neural responses at each of 102 sensor positions, we integrated a VEF of a latitudinal gradiometer with that of a longitudinal gradiometer at the same sensor position. This integration was performed by calculating a vector norm of the two VEFs at every time point (Noguchi et al. 2015; Suzuki et al. 2014), as shown by

$$\sqrt{x_i^2 + y_i^2}$$

, where x and y indicated MEG signals (fT/cm) in the latitudinal (x) and longitudinal (y) gradiometers at the sensor position i (1-102). In those vector-norm VEFs, a strong MEG response is shown as an upward deflection of the waveforms.

Source estimations of MEG signals

We estimated three-dimensional source locations of MEG signals (**Fig. 2B** and **Fig. 3B**) by the multiple sparse priors (MSP) approach (Friston et al. 2008) implemented in Statistical Parametric Mapping 5 (SPM5). Detailed procedures were described in our previous study (Noguchi et al. 2012). Briefly, we created a tessellated cortical mesh with 7,200 vertices for each subject using a template brain from the Montreal Neurological Institute (MNI). Positions of current dipoles (possible sources for MEG signals) were limited to the cortical surface and they were placed at each node of the mesh. After a spatial co-registration of this dipole mesh with a sensor space of MEG, current source density (source strength) at each dipole on the mesh was estimated by the MSP approach for each time point. Those results of the first-level (within-subject) analysis were spatially smoothed (12 mm in full-width at half maximum) and then submitted to the second-level (group-level) analysis across all subjects. Differences in neural responses (MSP solutions) between conditions were statistically evaluated by voxel-wise *t*-tests (random-effect analysis) on SPM5. A threshold for significant difference was set at $p < 0.05$, corrected for multiple comparisons (FWE).

Functional connectivity analysis

Our analyses above revealed two key regions (the right occipito-temporal and parietal areas) showing the RS to the canonical proportion (see **Results**). Based on those results, we investigated a functional connectivity between the two regions, to infer a model of neural pathway(s) for perception of the golden ratio. If no connectivity is found, for example, this would indicate an independence of the two regions, suggesting two separate pathways (one in the dorsal and another in the ventral) for the processing of golden ratio (parallel-processing model). If we find a significant connectivity between the right occipito-temporal and parietal

areas, however, it would suggest a neural pathway linking the two regions. Different types of RS in **Figure 2** and **Figure 3** (see **Results**) therefore reflect two stages of neural processing *within* a single pathway for aesthetic perception (serial-processing model).

Although many methods have been proposed for analyzing a functional connectivity (Kida et al. 2015), we simply computed correlation coefficients of MEG waveforms between the occipito-temporal and parietal regions. First, we divided all 102 sensors into 26 areas (see **Fig. 2A** for a configuration of the 26 areas). Waveforms at 4 (or 2) sensors within the same area were averaged together (the areal-mean waveform) (Suzuki et al. 2014). We then chose two areas, one representing the right occipito-temporal region (**Fig. 2A**) and another representing the right parietal region (**Fig. 3A**). Both of those areas showed distinct RS to the canonical proportion (see **Results**). Functional connectivity between the two areas was investigated by computing correlation coefficients of the areal-mean waveforms. We divided 850 data points (-100 to 750 ms) of a waveform into 17 epochs of 50 ms, obtaining a correlation coefficient for each epoch. A total of 17 coefficients were thus computed for each pair of areal-mean waveforms. These procedures of the correlation analysis were repeated for each condition and each subject.

As described above, we hypothesized a neural network for the processing of visual beauty linking the right occipito-temporal and parietal regions. Such pathway would be evidenced by a higher correlation of neural waveforms in responses to canonical than non-canonical sculptures. Statistical comparisons of correlation coefficients were thus made between those two (canonical vs. non-canonical) conditions. Specifically, we focused on raw (non-filtered) MEG waveforms to the first stimulus (S1) in each trial. Those S1 waveforms were not influenced by a S1-S2 interaction (e.g. RS) and thus can be used for a direct comparison of the canonical and non-canonical conditions. In **Figure 4**, correlation coefficients of neural responses to S-S-1 (S1 images in S-S trials) and D-S-1 (S1-images in

D-S trials) were integrated and labeled as “prototype (canonical)” condition, while those to S-D-1 and D-D-1 were labeled as “deformed (non-canonical)” condition. Waveforms to S-S-def-1 were not used for the correlation analysis to equate numbers of trials between the two conditions.

In addition to a main comparison above, we evaluated a significance of correlation coefficients by a permutation approach. In this approach, a sequence of 850 data points in an areal-mean waveform (from -100 to 750 ms) was changed into a random order (permutation). Correlation coefficients in each condition of each subject were computed on a pair of those permutated waveforms (dummy data) and then submitted to a group-level (N = 20) average. Repeating those procedures for 3,000 times generated a distribution of group-level correlation coefficients under a hypothesis of null effect. We determined a threshold for significance by identifying 5%-tails (2.5 % at the upper end) of this distribution. This approach revealed that the significance threshold in the present dataset was 0.0625 (a dotted line in **Fig. 4**), meaning that a correlation coefficient above 0.0625 (or below -0.0625) can be considered as significant with an error rate of $p < 0.05$.

A questionnaire after the MEG measurement

After MEG measurements, we asked subjects to complete a questionnaire about their knowledge and experience on art (presence/absence of professional training or education, etc.). Structures and items of this questionnaire were based on a previous study (Furnham and Walker 2001) and were identical to ones in our previous study (Noguchi and Murota 2013). Briefly, we asked subjects (i) how much they had studied art (Art studied, 1: junior-high level – 3: undergraduate level or higher), (ii) how much they had studied the history of art (History of art), (iii) how often they had visited art galleries in the previous year (Galleries past, 0: not at all – 4: once a week), (iv) how often they intended to go in the next year (Galleries future),

(v) the rate of trips to galleries on which the participants actively intend to go (Positiveness, 0: none – 4: always), and (vi) a rank (priority) of an art-related activities (e.g. visiting an art museum) among 10 leisure options (e.g. camping and drinking) on a free day (Activities, 0: art-related activities at the bottom of a list – 9: top priority). We then assessed their knowledge and memory of art with an objective test. For each of nine well-known sculptures (e.g., The Thinker by Rodin), subjects were asked to provide a name of an artist, title, the year (century) in which it was made (knowledge score, maximum: 27), and answered whether they had seen the sculpture before (memory score: maximum: 9). As a control group of subjects, we also asked experts in art (18 graduates and undergraduates majoring in the history of art at Kobe University, Japan) to fill out the same questionnaire. Scores of those expert students are compared with those of MEG subjects (non-experts) in **Figure 1E**. In the final section of the questionnaire, we checked whether MEG subjects had been aware of a purpose and manipulations in the present study. Subjects were asked to report if they had felt something odd on sculpture images during MEG measurements.

Results

Behavioral data (ratings of an aesthetic judgment)

Figure 1D displays ratings of an aesthetic judgment on S2 during MEG measurements. We first investigated whether subjects distinguished canonical sculptures from deformed ones by comparing ratings between the four conditions from S-S to D-D (with canonical S2) and S-S-def (with deformed S2). Mean ratings across the four conditions from S-S to D-D were 2.83 (across-subject SE: 0.12). A paired *t*-test between those mean ratings and ratings in S-S-def condition (mean: 2.54, across-subject SE: 0.12) yielded a significant difference ($t(19) = 4.41$, $p = .0003$, $d = 0.528$), indicating that subjects differentiated canonical and deformed sculptures when they were presented as a task-relevant stimuli (S2).

We then analyzed an effect of a repetition of the same sculpture as S1 and S2 (sculpture factor) and an effect of a repetition of the same proportion as S1 and S2 (proportion factor) on aesthetic ratings, using data in the four conditions (S-S to D-D). A repeated-measures analysis of variance (ANOVA) of the sculpture factor (same sculpture / different sculptures) × the proportion factor (same proportion /different proportions) yielded a significant main effect of the sculpture factor ($F(1,19) = 15.24$, $p = .001$, $\eta^2 = .445$), although no main effect of the proportion factor ($F(1,19) = .536$, $p = .473$, $\eta^2 = .027$) or interaction ($F(1,19) = .047$, $p = .83$, $\eta^2 = .002$) was observed. The significant effect of sculpture factor (S-S and S-D < D-S and D-D) showed that subjects provided higher ratings when two different sculptures were presented as S1 and S2 compared to when the same sculpture was repeated. On the other hand, the lack in the main effect of proportion factor indicated that a repetition of the same proportion between S1 and S2 did not affect aesthetic ratings on S2. Taken together, those results suggested that subjects discriminated the canonical from non-canonical proportions for task-relevant (S2) stimuli, while they did *not* so for task-irrelevant (S1) stimuli..

Neural suppression in the right occipito-temporal region

We first investigated a neural suppression effect induced by a repetition of the same sculpture image with the canonical proportion (S-S vs. S-D). **Figure 2A** shows neuromagnetic responses to S2 in S-S trials (S-S-2, blue) and S2 in S-D trials (S-D-2, red) averaged across all subjects. To obtain an overview of VEFs at 102 sensor positions, we divided them into 26 areas (25 areas with four sensor positions and one area with two sensor positions). Vector-norm VEFs at four or two sensor positions within the same area were averaged together (Suzuki et al. 2014). As shown by black rectangles in **Figure 2A**, a neural suppression (S-S-2 < S-D-2) was mainly seen in posterior regions of the right hemisphere at a latency of around 200 ms. Results of the MSP analysis (**Fig. 2B**) indicated that anatomical

sources of this neural suppression were located in the right occipito-temporal region. Typical vector-norm VEFs at a sensor in this region were enlarged in **Figure 2C** (background shadings denote SEs across all subjects). While the first neuromagnetic response at a latency of 100 ms (M1 response) was equally observed in S-S-2 (blue) and S-D-2 (red), a repetition of the same sculpture in S-S trials caused a selective attenuation of the second neuromagnetic responses at around 200 ms (M2 response). Those results were consistent with previous literature that a repetition suppression is primarily seen in neural responses from the higher than lower visual areas (Noguchi et al. 2004; Schacter and Buckner 1998). The same suppression effect was also seen when we compared VEFs to S1 (magenta) with those to S2 (blue) in the S-S trials (a comparison between S-S-1 and S-S-2, **Fig. 2D**).

An important point was whether this neural suppression reflected a repetition of an identical visual stimuli (visual RS) or a repetition of the canonical proportion (proportion-based RS). We thus compared neuromagnetic responses to S1 and S2 in S-S-def trials (**Fig. 2E**). If the suppression in **Fig. 2A-D** resulted from the visual RS, it should be also observed in this comparison between S-S-def-1 vs. S-S-def-2 (because an identical sculpture image with a deformed proportion was repeatedly shown in S-S-def trials). No significant suppression was observed in **Fig. 2E**, which indicated that suppression of M2 response in S-S-2 (**Fig. 2A-D**) reflected a repetition of the canonical proportion rather than a repetition of same visual image.

Neural suppression in the right parietal region

A hallmark of the golden ratio is that it defines a feature (or a rule) commonly embedded in various masterpieces such as *Venus de Milo* and *Doryphoros*, etc. Our working hypothesis was that some regions in the human brain may encode and react to this abstract rule independent of shapes and identities of individual sculptures. To explore such regions, we

contrasted neuromagnetic responses to S2 between D-S and D-D trials. Since both types of trials involved two different sculptures as S1 and S2, attenuated S2 responses in D-S than D-D would reflect the higher-level RS beyond sculpture identities.

As shown in **Figure 3A and 3B**, this type of suppression (identity-independent RS) was prominent in the right parietal region. Statistical significance of this RS was evaluated by point-by-point *t*-tests in VEFs between D-S-2 and D-D-2 (lower panel of **Fig. 3C**). To avoid a problem of multiple comparisons, we used the cluster-based permutation approach proposed in previous studies (Cichy et al. 2014; Maris and Oostenveld 2007; Nichols and Holmes 2002). These analyses demonstrated a significant ($p < 0.05$) suppression of neural activity in D-S-2 compared to D-D-2. It should be noted that the cluster-based approach used here was highly conservative, because of its priority on controlling family-wise error rate (Maris and Oostenveld 2007). Indeed, a size of significant time cluster in the present dataset was 112 ms (from 258 – 370 ms), corresponding to 112 consecutive time points with significant ($p < 0.05$) difference between D-S-2 and D-D-2.

Functional connectivity between the right occipito-temporal and parietal regions

Our analyses on RS revealed two key regions (regions of interest, ROIs) for the processing of the canonical proportion. A remaining question is whether those two regions were interconnected or not. We thus analyzed a functional connectivity between areal-mean waveforms in the two ROIs. Of particular interest was the connectivity at around 300 ms after a stimulus onset when the right parietal cortex showed a high-level (identity-independent) RS, possibly based on a low-level (identity-dependent) RS in the occipito-temporal cortex.

Figure 4 shows the functional connectivity (correlations) between the right occipito-temporal and parietal region at 250-300 and 300-350 ms. In both epochs, we found stronger connectivity when canonical (prototype) sculptures were presented as S1 (S-S-1 and

D-S-1) than when deformed sculptures were presented (S-D-1 and D-D-1). A repeated-measures ANOVA of stimulus (prototype/deformed) × epoch (250-300/300-350 ms) yielded a significant main effect of stimulus ($F(1,19) = 8.378$, $p = 0.009$, $\eta^2 = 0.306$). No main effect of epoch ($F(1,19) = 0.738$, $p = 0.401$, $\eta^2 = 0.037$) or an interaction ($F(1,19) = 0.584$, $p = 0.454$, $\eta^2 = 0.030$) was observed. The correlation in the prototype condition was especially high at 250-300 ms, exceeding a significance threshold (0.0625) estimated through the permutation method (see **Materials and Methods**). Those results indicate a neural network linking the two ROIs that is specialized for the processing of the canonical proportion. Different types of RS in **Figure 2** and **Figure 3** thus would reflect two stages of neural processing *within* a single pathway for aesthetic perception, rather than two separate pathways independently processing the aesthetic information.

An effect of stimulus repetitions across experimental sessions

As shown in **Fig. 1C**, we repeatedly presented the same set of sculpture images (*A-Z* and *A'-Z'*) over the six experimental sessions. An effect of this repetition (across-session repetition) on MEG waveforms was examined in **Figure 5**. We compared the RS in the right parietal cortex between the first two sessions (session 1&2) and the last two sessions (session 5&6). As shown in **Figure 5A**, the identity-independent RS (D-S-2 < D-D-2) was observed both in session 1&2 and 5&6. A repeated-measures ANOVA of trial type (D-S-2/D-D-2) × and session (1&2/5&6) on mean amplitudes at 258 – 370 ms (**Fig. 5B**) yielded a significant main effect of trial type ($F(1,19) = 9.737$, $p = 0.006$, $\eta^2 = 0.339$). No main effect of session ($F(1,19) = 0.341$, $p = 0.566$, $\eta^2 = 0.018$) or an interaction ($F(1,19) = 0.483$, $p = 0.495$, $\eta^2 = 0.025$) was observed. Those data indicate that repeated presentations of the same stimuli did *not* affect the RS in the present study.

Behavioral data (a post-experimental questionnaire)

Scores of the questionnaire on art knowledge and experiences are shown in **Fig. 1E**. For all items, significant differences in scores were observed between the experts and MEG subjects ($t(36) > 3.72$, $p < 0.001$, $d > 1.20$ for all). These data indicated that subjects in the present MEG experiment had no professional experience in art.

At the final section of the questionnaire, we asked subjects an open-ended question whether they had felt anything odd about sculpture images. Although most subjects did not refer to a proportion of sculptures, one subject reported "strange-balanced bodies in 1-25 % of the stimuli". We thus re-performed all MEG analyses with data of this subjects excluded, confirming no change in results on this (N = 19) dataset.

Discussion

In the present study, we investigated the neural adaptation effect induced by a repetitive presentation of sculpture(s) with the canonical proportion. The RSs were mainly observed in the right (rather than left) hemisphere, probably because of the right-hemispheric dominance for the visual processing of human body images (Downing et al. 2006). The first type of RS emerged from the occipito-temporal region at a latency of about 200 ms. This region showed reduced activity when the same sculpture with the canonical proportion was repeated (S-S) compared to when not (S-D). Furthermore, we found another type of RS in the right parietal region at around 300 ms. In this region, the RS to the canonical proportion was observed even when sculptures with different identities were presented as S1 and S2 (D-S < D-D). This identity-independent RS was a novel approach in the present study, because a factor of identity had been strictly controlled in previous studies using the same set of sculptures between the canonical and deformed conditions (Di Dio et al. 2007; Noguchi and Murota 2013). Our data overall indicated two systems (stages) for the processing of aesthetic

information in the brain that are dissociated in both spatial (occipito-temporal vs. parietal) and temporal (latency: 200 ms vs. 300 ms) dimensions.

The occipito-temporal areas are generally known as a core region in the ventral pathway. Neurons in this pathway show selective responses to specific colors (Komatsu and Ideura 1993) and/or shapes (Fujita et al. 1992). The RS in the present study (**Fig. 2**) thus would reflect neural processing for the shape information of sculptures. It is notable that the RS was selectively induced by a repetition of the canonical proportion (S-S), not by a repetition of a deformed proportion (S-S-def). Furthermore, we found that this RS by the canonical proportion started at less than 200 ms from an onset of images. Those results suggest a rapid response of our brain to aesthetic information, presumably in a feedforward (rather than feedback) pathway of visual processing. Our present data might be also consistent with a previous view that the ventral occipital region responds to beauty automatically (Chatterjee 2011).

The second type of RS related to the golden ratio was found in the parietal cortex. An involvement of the parietal region in aesthetic perception has been reported in a number of studies (Cela-Conde et al. 2009; Cupchik et al. 2009; Di Dio et al. 2007; Jacobsen et al. 2006). Some researchers argued that neural response in the parietal areas reflected attentional analysis of visual inputs (Cela-Conde et al. 2011) or a decision-making process for aesthetic judgments (Chatterjee 2011). Others proposed that this region was related to empathic nature of the relationship automatically established between artworks and beholders (Di Dio and Gallese 2009). A major finding in the present study was the prominent RS to the canonical proportion induced by two different sculptures (D-S < D-D), indicating that neural activity in this area encoded the golden ratio as a feature (or a rule) commonly embedded in many artworks. Our data thus showed that such high-level visual analyses of aesthetic information were actually performed in the non-experts' brain. One should note, however, that the RS in

the parietal region (D-S-2 < D-D-2) was not observed in behavioral data (ratings, D-S-2 = D-D-2, **Fig. 1D**), indicating that neural activity in this area did not represent final judgments of aesthetic evaluation. Some other regions in the brain (e.g. orbitofrontal cortex), therefore, might receive inputs from the parietal cortex, making a final decision of aesthetic judgments. Indeed, a number of visual factors have been known to affect our aesthetic perception, such as symmetry, colorfulness (or color harmony), and smoothness (Jacobsen et al. 2006; Palmer and Griscom 2013). Although we reported here neural responses of parietal and temporal regions to the golden ratio, it remains to be elucidated whether the same results could be obtained when other visual factors of beauty are manipulated. Further research would be necessary to reveal an entire picture of brain responses associated with aesthetic judgments.

In contrast to the RS in the occipito-temporal and parietal cortex, no RS was observed in the frontal cortex. This might be inconsistent with previous studies reporting an involvement of the anterior brain regions in aesthetic evaluation (Di Dio et al. 2007; Kirk et al. 2009; Lacey et al. 2011). One reason for this discrepancy would be a limited spatial resolution of MEG. Accurate source localization of neuromagnetic signals is generally difficult (i.e. ill-posed inverse problem), especially in the high-level brain regions with a complex neural circuit. Another reason for the lack of frontal activity was that we presently measured VEFs to sculpture images. Although the VEF analysis is useful to detect transient neural responses evoked by a sensory stimulus, it is less sensitive to sustained responses of neural activity that are frequently seen in the frontal cortex. A use of frequency analysis (e.g. Fourier transformation) might be helpful to cover this shortcoming of the VEF analysis.

We finally refer to several limitations in the present study. First, the familiarity of visual stimuli might not be sufficiently controlled in the present study. Although the deformation of sculpture images significantly lowered ratings in an aesthetic judgment (**Fig. 2**), it would simultaneously reduce the familiarity of those images. The RS in the present study thus might

reflect a repetition of familiar (non-deformed) images, not a repetition of the canonical proportion. We think this problem is related to a difficulty in dissociating beauty (or attractiveness) from familiarity. It is widely known that faces with average values of population were judged as attractive (Langlois and Roggman 1990), which is called the beauty-in-averageness effect (Winkielman et al. 2006). Repeated exposure of the individual to a stimulus enhanced his/her attitude toward it (the mere exposure effect) (Zajonc 1968). These data suggest a close relationship between familiarity and an aesthetic value of a stimulus (the more familiar, the more attractive). It is thus difficult to isolate beauty from familiarity, especially when human body parts are used as stimuli (Park et al. 2010). Presenting other categories of images, such as geometric shape, would resolve this issue, because familiarity was not necessarily correlated with attractiveness in those categories (Park et al. 2010). Another limitation of the present study was a use of the golden ratio. There has been a fierce debate over theoretical or empirical basis for the golden ratio or golden section. Some researchers provided the evidence against the golden section (Höge 1997), while others not (Schmid et al. 2008). It was thus important for us to check whether participants actually showed sensitivity to the golden ratio before analyzing their brain activity. Our behavioral data in **Figure 1D** showed higher aesthetic ratings for original (S-S-2, S-D-2, D-S-2, and D-D-2) than deformed (S-S-def-2) images, which ensured the sensitivity of our subjects to the canonical proportion. We thus presume that the RS reported in the present study was related to the neural processing of the golden ratio. It is unclear, however, whether those behavioral data reflected a universal preference of humans to a visual parameter of beauty (golden ratio) or subjective preferences of our participants acquired through their developmental and cultural factors. More studies would be necessary to elucidate whether there is a universal mechanism for the perception of beauty that is intrinsically built in the human brain.

Acknowledgements. We thank Mr. Y. Takeshima for his technical supports. This work was supported by KAKENHI Grants (22680022 and 26700011) from the Japan Society for the Promotion of Science (JSPS). The authors declare no competing financial interests.

References

Barron HC, Garvert MM, Behrens TE (2016) Repetition suppression: a means to index neural representations using BOLD? Philos Trans R Soc Lond B Biol Sci 371

Brainard DH (1997) The Psychophysics Toolbox. Spat Vis 10:433-436

Buckner RL et al. (1998) Functional-anatomic correlates of object priming in humans revealed by rapid presentation event-related fMRI. Neuron 20:285-296

Cela-Conde CJ, Agnati L, Huston JP, Mora F, Nadal M (2011) The neural foundations of aesthetic appreciation. Prog Neurobiol 94:39-48

Cela-Conde CJ et al. (2009) Sex-related similarities and differences in the neural correlates of beauty. Proc Natl Acad Sci U S A 106:3847-3852

Chatterjee A (2011) Neuroaesthetics: a coming of age story. J Cogn Neurosci 23:53-62

Chatterjee A, Vartanian O (2014) Neuroaesthetics. Trends Cogn Sci 18:370-375

Cichy RM, Pantazis D, Oliva A (2014) Resolving human object recognition in space and time. Nat Neurosci 17:455-462

Cupchik GC, Vartanian O, Crawley A, Mikulis DJ (2009) Viewing artworks: contributions of cognitive control and perceptual facilitation to aesthetic experience. Brain Cogn 70:84-91

Di Dio C, Gallese V (2009) Neuroaesthetics: a review. Curr Opin Neurobiol 19:682-687

Di Dio C, Macaluso E, Rizzolatti G (2007) The golden beauty: brain response to classical and renaissance sculptures. PLoS One 2:e1201

Downing PE, Chan AW, Peelen MV, Dodds CM, Kanwisher N (2006) Domain specificity in visual cortex. Cereb Cortex 16:1453-1461

Friston K et al. (2008) Multiple sparse priors for the M/EEG inverse problem. Neuroimage 39:1104-1120

Fujita I, Tanaka K, Ito M, Cheng K (1992) Columns for visual features of objects in monkey inferotemporal cortex. Nature 360:343-346

Furnham A, Walker J (2001) The influence of personality traits, previous experience of art, and demographic variables on artistic preference. Personality and Individual Differences 31:997-1017

Gagnepain P, Chetelat G, Landeau B, Dayan J, Eustache F, Lebreton K (2008) Spoken word memory traces within the human auditory cortex revealed by repetition priming and functional magnetic resonance imaging. J Neurosci 28:5281-5289

Grill-Spector K, Kushnir T, Edelman S, Avidan G, Itzchak Y, Malach R (1999) Differential processing of objects under various viewing conditions in the human lateral occipital complex. Neuron 24:187-203

Höge H (1997) The Golden Section Hypothesis — Its Last Funeral. Empir Stud Arts 15:233-255

Hayashi MJ et al. (2015) Time Adaptation Shows Duration Selectivity in the Human Parietal Cortex. PLoS Biol 13:e1002262

Hekkert P, VanWieringen PCW (1996) Beauty in the eye of expert and nonexpert beholders: A study in the appraisal of art. American Journal of Psychology 109:389-407

Henson R, Shallice T, Dolan R (2000) Neuroimaging evidence for dissociable forms of repetition priming. Science 287:1269-1272

Jacobsen T (2013) On the electrophysiology of aesthetic processing. Prog Brain Res 204:159-168

Jacobsen T, Schubotz RI, Hofel L, Cramon DY (2006) Brain correlates of aesthetic judgment of beauty. Neuroimage 29:276-285

Jenkins AC, Macrae CN, Mitchell JP (2008) Repetition suppression of ventromedial prefrontal activity during judgments of self and others. Proc Natl Acad Sci U S A 105:4507-4512

Kawabata H, Zeki S (2004) Neural correlates of beauty. J Neurophysiol 91:1699-1705

Kida T, Tanaka E, Kakigi R (2015) Multi-Dimensional Dynamics of Human Electromagnetic Brain Activity. Front Hum Neurosci 9:713

Kirk U, Skov M, Hulme O, Christensen MS, Zeki S (2009) Modulation of aesthetic value by semantic context: an fMRI study. Neuroimage 44:1125-1132

Komatsu H, Ideura Y (1993) Relationships between color, shape, and pattern selectivities of neurons in the inferior temporal cortex of the monkey. J Neurophysiol 70:677-694

Kourtzi Z, Kanwisher N (2001) Representation of perceived object shape by the human lateral occipital complex. Science 293:1506-1509

Lacey S et al. (2011) Art for reward's sake: visual art recruits the ventral striatum. Neuroimage 55:420-433

Langlois JH, Roggman LA (1990) Attractive Faces Are Only Average. Psychol Sci 1:115-121

Lau T, Cikara M (2017) fMRI Repetition Suppression During Generalized Social Categorization. Sci Rep 7:4262

Livio M (2003) The Golden Ratio: The Story of Phi, the World's Most Astonishing Number. Broadway Books, New York

Maris E, Oostenveld R (2007) Nonparametric statistical testing of EEG- and MEG-data. J Neurosci Methods 164:177-190

Miller EK, Li L, Desimone R (1991) A neural mechanism for working and recognition memory in inferior temporal cortex. Science 254:1377-1379

Mizokami Y et al. (2014) Difference in brain activations during appreciating paintings and photographic analogs. Front Hum Neurosci 8:478

Nadal M (2013) The experience of art: insights from neuroimaging. Prog Brain Res 204:135-158

Nadal M, Pearce MT (2011) The Copenhagen Neuroaesthetics Conference: prospects and pitfalls for an emerging field. Brain Cogn 76:172-183

Nakamura S (2002) Fibonacci-suu no microcosmos (Microcosmos of Fibonacci constant). Nippon Hyoron sha, Tokyo

Nichols TE, Holmes AP (2002) Nonparametric permutation tests for functional neuroimaging: a primer with examples. Hum Brain Mapp 15:1-25

Nishitani N, Hari R (2002) Viewing lip forms: cortical dynamics. Neuron 36:1211-1220

Noguchi Y, Inui K, Kakigi R (2004) Temporal dynamics of neural adaptation effect in the human visual ventral stream. J Neurosci 24:6283-6290

Noguchi Y, Kimijima S, Kakigi R (2015) Direct behavioral and neural evidence for an offset-triggered conscious perception. Cortex 65:159-172

Noguchi Y, Murota M (2013) Temporal dynamics of neural activity in an integration of visual and contextual information in an esthetic preference task. Neuropsychologia 51:1077-1084

Noguchi Y, Yokoyama T, Suzuki M, Kita S, Kakigi R (2012) Temporal dynamics of neural activity at the moment of emergence of conscious percept. J Cogn Neurosci 24:1983-1997

Oldfield RC (1971) The assessment and analysis of handedness: the Edinburgh inventory. Neuropsychologia 9:97-113

Palmer SE, Griscom WS (2013) Accounting for taste: individual differences in preference for harmony. Psychon Bull Rev 20:453-461

Park J, Shimojo E, Shimojo S (2010) Roles of familiarity and novelty in visual preference judgments are segregated across object categories. Proc Natl Acad Sci U S A 107:14552-14555

Pelli DG (1997) The VideoToolbox software for visual psychophysics: transforming numbers into movies. Spat Vis 10:437-442

Schacter DL, Buckner RL (1998) Priming and the brain. Neuron 20:185-195

Schmid K, Marx D, Samal A (2008) Computation of a face attractiveness index based on neoclassical canons, symmetry, and golden ratios. Pattern Recognition 41:2710-2717

Suzuki M, Noguchi Y, Kakigi R (2014) Temporal dynamics of neural activity underlying unconscious processing of manipulable objects. Cortex 50:100-114

Vessel EA, Starr GG, Rubin N (2013) Art reaches within: aesthetic experience, the self and the default mode network. Front Neurosci 7:258

Wiggs CL, Martin A (1998) Properties and mechanisms of perceptual priming. Curr Opin Neurobiol 8:227-233

Winkielman P, Halberstadt J, Fazendeiro T, Catty S (2006) Prototypes are attractive because they are easy on the mind. Psychol Sci 17:799-806

Winston AS, Cupchik GC (1992) The evaluation of high art and popular art by naive and experienced viewers. Vis Arts Res 18:1-14

Zajonc RB (1968) Attitudinal Effects of Mere Exposure. Journal of Personality and Social Psychology 9:1-27

Zeki S (1999) Art and the brain. J Conscious Stud: Controvers Sci Humanit 6:76-96

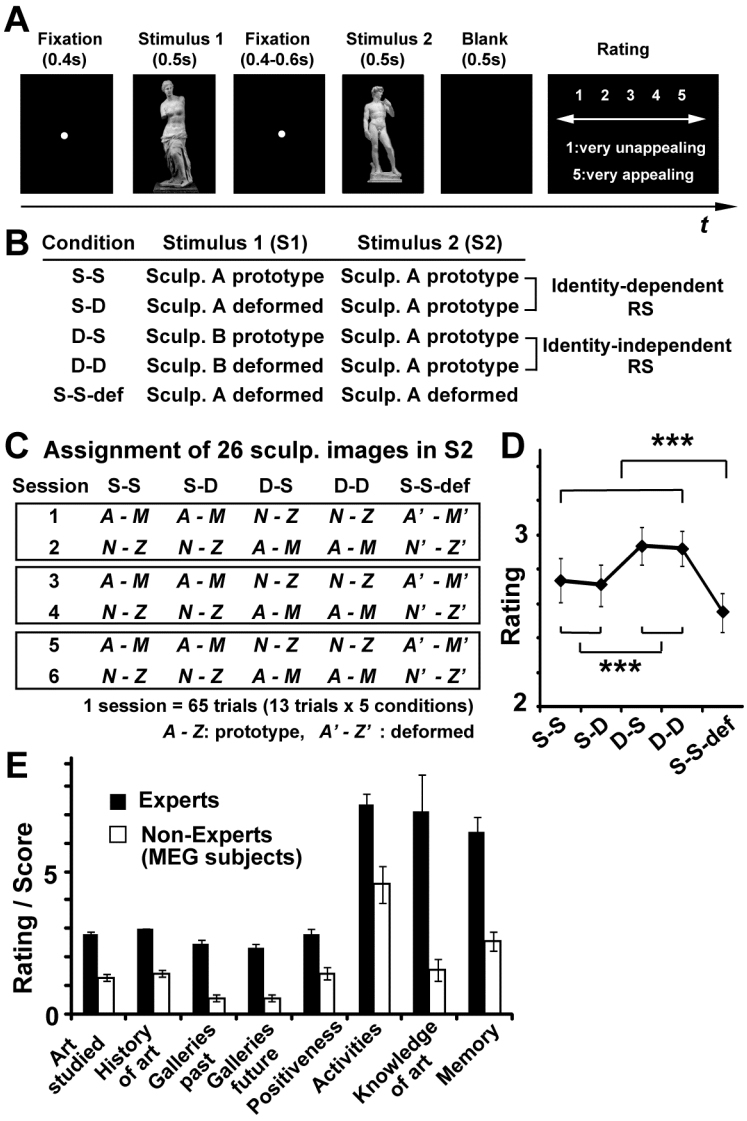

Fig. 1 Experimental designs and behavioral data. (**A**) Structures of one trial. Two images of sculpture(s), called S1 and S2, were sequentially presented in the central visual field. Subjects performed an aesthetic rating on S2, neglecting S1. (**B**) Structures of 5 conditions. In same-sculpture same-proportion (S-S) trials, an identical image of a sculpture with the golden proportion (e.g. *David di Michelangelo*) was repeatedly presented as S1 and S2. The canonical proportion of S1 was deformed (either into a short-leg or long-leg proportion) in S-D (same-sculpture different-proportion) trials. The third condition involved two different sculptures (e.g. *Venus de Milo* as S1 and *David* as S2, as **Fig. 1A**), both of which had the golden proportion (different-sculpture same-proportion or D-S trials). The golden proportion of S1 was impaired in the fourth condition (different-sculpture different-proportion or D-D

trials). The last condition (S-S-def) served as a control in which the same sculpture with a deformed proportion was repeatedly presented. A neural suppression induced by a repetition of the canonical proportion would be seen as differential MEG responses to S2 between S-S vs. S-D trials or between D-S vs. D-D trials. Especially, the suppression in D-S vs. D-D would represent the higher-level processing that encodes and reacts to the golden ratio shared by different sculptures (S1 and S2). (**C**) The assignment of sculpture images in S2 (second stimulus in each trial). The *A –Z* indicate 26 images of the canonical proportion used in the present study, while *A'-Z'* denote their deformed versions. In session 1 (65 trials), we presented 13 images from *A-M* as S2 in S-S and S-D trials and the other 13 images (*N-Z*) in D-S and D-D trials. This assignment was reversed in session 2. As a whole experiment (session 1-6), 78 trials in a given condition (e.g. S-S) consisted of three repetitions of 26 images. (**D**) Results of the aesthetic rating on S2 during MEG measurements. In these and subsequent figures, all error bars denote standard errors (SEs) across participants. (**E**) Results of a post-experimental questionnaire on knowledge and experience of art. Data of participants in an MEG experiment are shown as white bars (non-experts). Data of expert participants are taken from our previous study (Noguchi and Murota 2013) with permission from Elsevier. ***$p < 0.001$

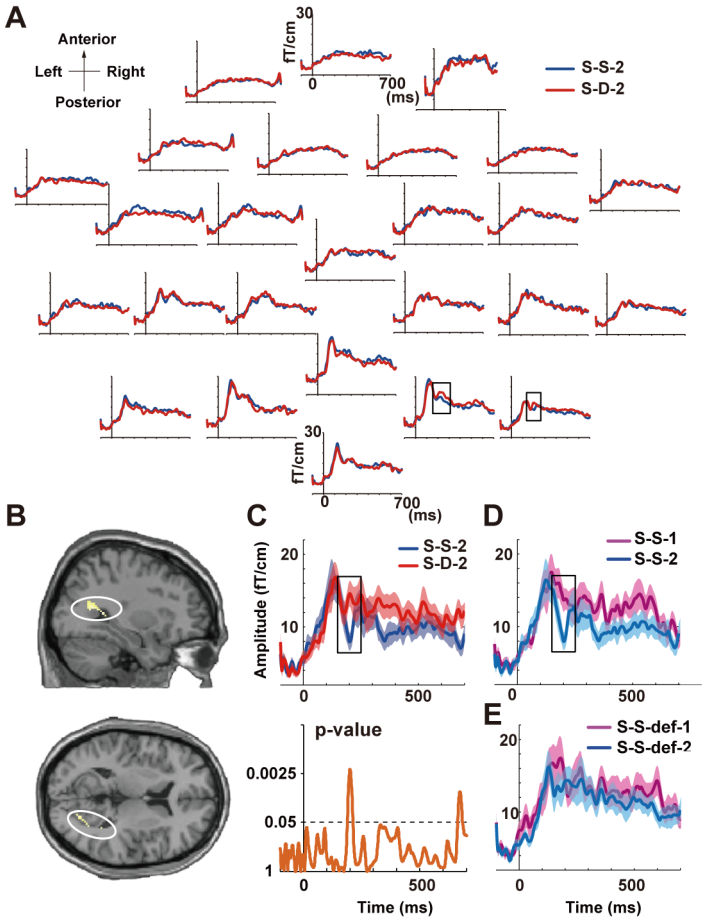

Fig. 2 Repetition suppression (RS) between S-S and S-D trials. (**A**) Visual-evoked fields (VEFs) induced by S2 image (S2-VEFs) averaged across all subjects. The waveforms recorded from anterior regions are plotted in the upper positions. We divided vector-norm VEFs at 102 sensor positions into 26 groups. The VEFs belonging to the same group were averaged. The RS can be seen as attenuated response in S-S (blue) compared to S-D (red) trials (see black rectangles). Note that, in the vector-norm VEFs, a strong neuromagnetic response is always shown as an upward deflection of waveforms. (**B**) Results of MSP estimations (see **Materials and Methods**). Anatomical sources for the RS were located in the occipito-temporal regions in the right hemisphere. (**C**) Vector-norm VEFs to S2 in S-S and S-D trials (S-S-2 and S-D-2, respectively) at a typical sensor in the right occipito-temporal region. In this and subsequent figures, background shadings indicate SEs across all subjects.

The RS was mainly seen in the M2 component of VEF (Noguchi et al. 2012) at a latency of around 200 ms. Changes in *p*-values of point-by-point *t*-tests (S-S-2 vs. S-D-2) are shown in the lower panel. (**D**) Vector-norm VEFs to S1 in S-S trials (S-S-1) and S2 in S-S trials (S-S-2) at the same sensor position. (**E**) Vector-norm VEFs to S1 in S-S-def trials (S-S-def-1) and S2 in S-S-def trials (S-S-def-2). The RS was mainly induced by a repetition of the golden ratio between S1 and S2 (**C** and **D**), not by a repetition of the same visual images (**E**).

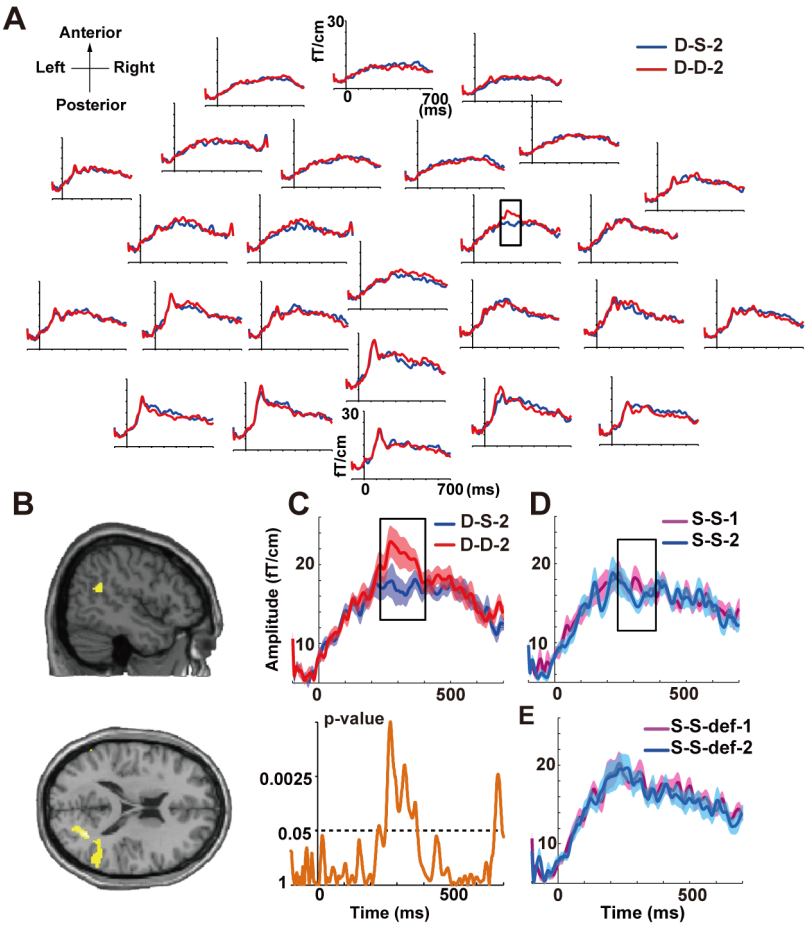

Fig. 3 RS between D-S and D-D trials. (**A**) VEFs induced by S2 in D-S (blue) and D-D (red) trials. The higher-level RS induced by the golden ratio in two different sculptures (identity-independent RS) was seen (black rectangle). (**B**) Result of MSP source estimations for the RS (D-S-2 < D-D-2). (**C**) An enlarged display of VEFs in the right anterior-parietal areas. Waveforms at four sensors positions were averaged. (**D**) A comparison of S-S-1 and S-S-2. (**E**) A comparison of S-S-def-1 and S-S-def-2. The right parietal region showed the RS induced by a repetition of the golden ratio (**D**) rather than a repetition of the same visual inputs (**E**), as the right occipito-temporal region in **Figure 2**.

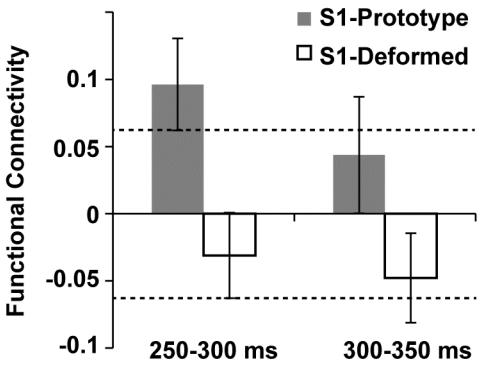

Fig. 4 Results of the functional connectivity analysis. Neuromagnetic responses in the right occipito-temporal region were strongly correlated with those in the right parietal region when a canonical sculpture was presented as S1 (S1-Prototype, gray bars) compared to when not (S1-Deformed, white bars). The connectivity was especially strong at 250-300 ms after the S1 onset, higher than a significance threshold (dotted lines) estimated by the permutation methods (see **Materials and Methods**).

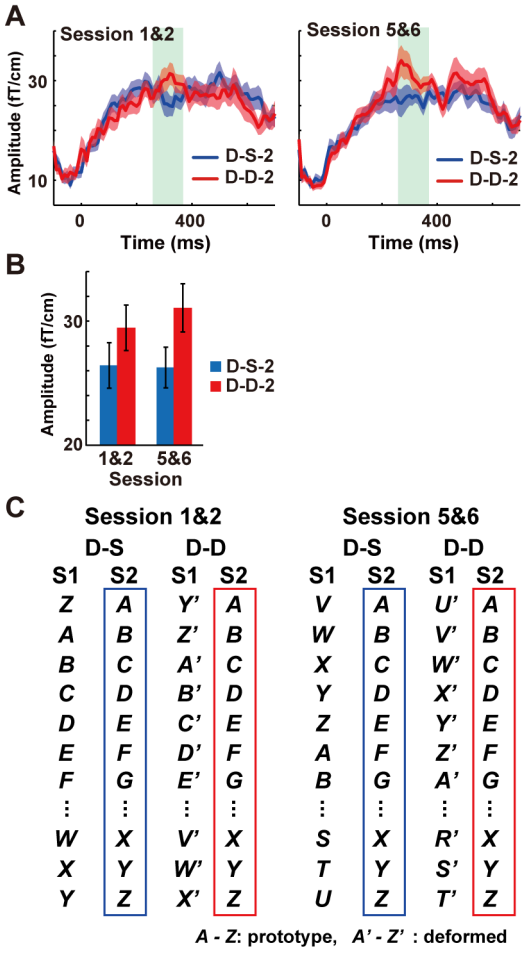

Fig. 5 Comparisons of S2-VEFs between the first and last sessions. (**A**) Identity-independent RS (D-S-2 < D-D-2) in session 1&2 (left) and session 5&6 (right). Gray backgrounds denote time periods in which the significant RS was seen in **Fig. 3** (258 – 370 ms). (**B**) Mean amplitudes of VEFs from 258 to 370 ms. A two-way ANOVA yielded a significant main effect of a trial type (D-S-2 < D-D-2). (**C**) Parings of S1 and S2 images in D-S and D-D trials in session 1&2 (left) and 5&6 (right). The *A –Z* and *A'-Z'* indicate 26 images with the canonical and deformed proportions, respectively. Note that S1-S2 pairings were completely different across four conditions (D-S in session 1&2, D-D in session 1&2, D-S in session 5&6, D-D in session 5&6). The main effect in panel **B** (D-S-2 < D-D-2 in both session 1&2 and 5&6) thus cannot be explained by a difference in S1-S2 pairings across the four conditions.